JOURNAL OF SPACECRAFT AND ROCKETS
Vol. 42, No. 1, January–February 2005

Mission and Constellation Design for Low-Cost Weather Observation Satellites

Chung-Hsien Lin*
National Central University, Chung Li 320, Taiwan, Republic of China
and
Zuu-Chang Hong†
Tamkang University, Taipei 25137, Taiwan, Republic of China

The mission and constellation design for acquiring weather images of Taiwan, Republic of China, is presented. The mission requires acquiring at least one image covering Taiwan per hour. The constellation is constituted of the low-cost microsatellites, which employ a passive magnetic attitude control system and an imagery system of miniature cameras. The coverage requirements, accessible coverage zone, access coverage, and access coverage gap, are defined according to the constellation design. The Walker constellation method is employed to calculate the minimum satellites in constellation for the mission requirements. The calculation result shows that the 14/14/0 constellation satisfactory meets the mission requirement. The 14/14/0 constellation is also extended to acquire the images of targets located in the certain specified geomagnetic latitude band (−5 to 22 deg) hourly, with a slight modification of imagery system of each satellite by using multicameras. An application to observe a typhoon as the moving target having 127 images acquired in 102 h in the warning area of Taiwan is also presented.

Nomenclature

AZ, $A'Z'$	=	accessible coverage zone
B_j	=	geomagnetic latitude bands
B_{la}	=	latitude band between ±33 deg
B_s	=	intersection of B_u and B_{la}
B_u	=	union of B_j
B_w	=	warning area
F	=	relative phasing parameter, $360/T$ deg
G_k	=	access coverage gap, min
$G_{\max}$, G_{mean}	=	maximal and mean access coverage gap, min
i	=	common inclination for all satellites, deg
L_h,	=	height of accessible coverage zone in latitude, °N
L_w	=	width of accessible coverage zone in longitude, °E
m, n	=	mth and nth sample point along the longitudinal and latitudinal directions, respectively, over the accessible coverage zone
P	=	number of commonly inclined orbital planes
S_j	=	camera sets
T	=	total number of satellites in constellation
z	=	body axis of satellite
β	=	setup angle of charge-coupled device, deg
θ_{g1}, θ_{g2}	=	geographic longitude and latitude, °
θ_{m1}, θ_{m2}	=	geomagnetic longitude and latitude, °
Φ_0	=	reference pointing error, deg
$\Phi_{0\max}$, $\Phi_{0\text{mean}}$	=	maximal and mean reference pointing error, deg
ψ	=	angle of field of view, deg
Ω	=	misalignment from the z axis to the local field direction, deg

Subscripts

$g1$, $g2$	=	geographic longitude and latitude
j	=	number of camera sets and geomagnetic bands
k	=	number of gaps
$m1$, $m2$	=	geomagnetic longitude and latitude
max	=	maximal
mean	=	mean
s	=	intersection
u	=	union
w	=	warning
0	=	reference

Introduction

IN recent decades, more space research programs in universities are focused on the development of micro- or nanosatellites, which are designed as the secondary payload of most space vehicles. The main goal of these programs is to educate students in the design, manufacturing, integration, and operation of a real satellite. These programs also demonstrate the way in which the satellites can be built quickly and inexpensively, with minimal industry support and provide resources for both scientific research and educational purposes. To achieve these purposes, some space programs attempt to employ a simple attitude control system and off-the-shelf components as onboard payloads. For instance, some satellites employed a passive magnetic attitude control system and the charge-coupled device (CCD) camera to obtain the Earth images. Examples include WO-18,[1] SAPPHIRE,[2] Spartnik,[3] MUNIN,[4] and TUUSAT.[5]

The CCD mission of TUUSAT was to acquire the weather images covering Taiwan, which is located in the cyclone tropic. The weather changes rapidly during typhoon season, and the weather images are valuable for meteorologists and weather forecasting to predict the dynamic trend of typhoons. However, the CCD mission of TUUSAT is designed to acquire only one image per day in the daylight hours. For weather forecasting, the satellite should provide more images in a shorter time interval for the real-time weather analysis. For instance, the geostationary weather satellite GMS-5 can provide several images per hour. A low-Earth-orbit constellation of similar satellites shall provide more amounts of weather images everyday.

The first effort of this paper concerns the constellation design for acquiring weather images of Taiwan hourly. Each satellite in constellation contains the similar attitude control system and imagery system as that of TUUSAT. The method of Walker constellation

Received 18 August 2003; revision received 15 November 2003; accepted for publication 23 December 2003.

*Graduate Student, Department of Mechanical Engineering.
†Professor, Department of Mechanical and Electro-Mechanical Engineering, Tamsui. Associate Fellow AIAA.

is also employed to calculate the minimum number of satellites. The result of this constellation design for picture taking hourly of weather images of Taiwan will be extended to observe a specified geomagnetic latitude band of −5 to 22 deg. An application to observe a typhoon as moving target within a warning area including Taiwan will be also presented.

Imagery System

Similar to the imagery system in Ref. 5, the present system of each satellite contains two miniature cameras, and the angle ψ of field of view (FOV) of each camera is 100 deg. The two cameras are set up each on the opposite side of the lateral of satellite with the optimal setup angle β, which is the angle between the spin axis (z axis) and the camera line of sight. This setup angle is determined by the corresponding minimum values of the distributions of $\Phi_{0\max}$ and $\Phi_{0\text{mean}}$[5]; both appeared as functions of β:

$$\Phi_{0M}(\beta) = \sqrt{\frac{\sum_{m=1}^{m}\sum_{n=1}^{n}\Phi_{0m,n}^{2}(\beta)|_{\beta}}{m \times n}} \tag{1}$$

$$\Phi_{0\max}(\beta) = \max[\Phi_{0\,m,n}(\beta)|_{\beta}] \tag{2}$$

The pointing error is defined as the angle between the camera line of sight and the position vector from the satellite to the target. The parameter Φ_0 is defined as the pointing error under the assumption that the misalignment Ω between the z axis and the local field direction is zero. Usually Ω varies from 0 to 10 deg as given in Refs. 6 and 7. In Eqs. (1) and (2), $\Phi_{0\,m,n}$ represents Φ_0 when the imaging logic is met at the mth and nth sample point over a specified area (given as the accessible coverage zone next). Here, m and n are the number of sample points with equal spacing over this specified area along the longitude and latitude directions, respectively.

The imaging requirement of imagery system is defined as that the images must cover Taiwan or Taiwan must be within the FOV of camera as it is triggered. The mathematic expression[5] of the imaging requirement is given by

$$\Phi_0 \le (\psi/2) - \Omega \tag{3}$$

In the preceding equation we take Ω as maximum of 10 deg, and then the maximum value of Φ_0 must be less than 40 deg to meet the imaging requirement. Because the images are acquired hourly throughout day and night (instead of only in daylight hours in Ref. 5), the near infrared filters are employed to distinguish the clouds, the ground, and the ocean. The passive CCD imaging logic and its implementation scheme,[5] which determines the proper timing of shooting images, is adopted in the present design.

Constellation Design

The coverage requirements are accessible coverage zone, access coverage, and access coverage gap.[8] The accessible coverage zone is defined as the area in which the imagery systems of satellites have opportunities to acquire the images covering Taiwan. The imagery system and the imaging logic are designed according to the operating orbit and the attitude motion of satellite. In Ref. 5, the spacecraft was assumed to operate at a sun synchronous orbit with 98.6-deg inclination and 800-km altitude. To correspond to the imagery system design in Ref. 5, the same sun-synchronous orbit is adopted here. The accessible coverage zone is designed as the areas AZ and AZ′, which are centered at Taiwan with height L_h and width L_w as shown in Fig. 1. Here, L_h is the length of the footprint in latitude when the satellite spins half of a revolution with the minimal spin rate, which is 0.05 rpm according to the simulation result of passive attitude control system in Refs. 6 and 7. The points A, B′, C′, D, lie on the edge of the local horizon of Taiwan. The solid lines $\overline{AB}$, $\overline{CD}$ and the dashed lines $\overline{A'B'}$, $\overline{C'D'}$ represent the footprints that the satellite ascends from south to north and descends from north to south, respectively. Here, the implementation of CCD imaging logic is modified by substituting AZ and AZ′ to the shooting zone defined in Ref. 5. When the satellite is ascending, the area AZ is adopted in the CCD imaging logic, and when the satellite is descending AZ′ is adopted. When AZ and AZ′ are applied to the CCD imaging logic, the calculated distributions of $\Phi_{0\max}$ and Φ_{0M} ($m = 36$, $n = 36$) of Taiwan are shown in Fig. 2. It shows that the minimum $\Phi_{0\max}$ appears at $\beta = 66$. When $\beta = 66$ is selected, the maximal reference pointing error is 35 deg and satisfies the imaging requirement in Eq. (3).

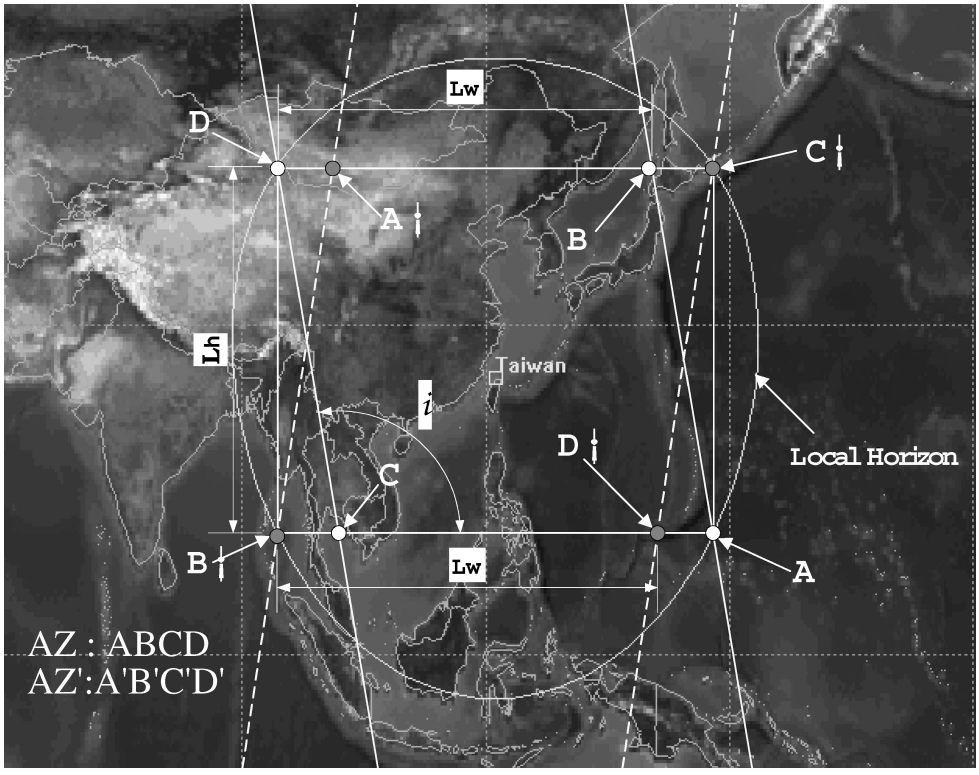

Fig. 1 Accessible coverage zone.

The access coverage is defined as the access time to the accessible coverage zone. The access coverage starts when the footprint of satellite ascends to $\overline{AC}$ or descends to $\overline{A'C'}$ and stops when it ascends to $\overline{BD}$ or descends to $\overline{B'D'}$. The access coverage gap is defined as the revisit time between two adjacent access coverages, that is, from the time that the current access coverage stopped to the time that the next access coverage started. It is evident that access coverage is 10 min (spin time for half of a revolution). The access coverage gap should be less than one hour in order to meet the mission requirements. To estimate the minimum satellites required in constellation, two parameters are given as

$$G_{\max} = \max(G_k) \tag{4}$$

$$G_{\text{mean}} = \frac{\sum_1^k G_k}{k} \tag{5}$$

To meet the coverage requirements, $G_{\max}$ must be less than one hour.

Walker Constellation

To use Walker's notation,[9] symmetric constellations of satellites can be described by the parameters $T/P/F$ and i. To have a symmetric arrangement, the T/P satellites in a given orbital plane are equally spaced in central angle (phasing), and the P orbital planes are evenly spaced through 360 deg of right ascension of ascending node. The phasing parameter F relates the satellite positions in one orbital plane to those in an adjacent plane (i.e., interorbit phasing). The units of F are $360/T$.

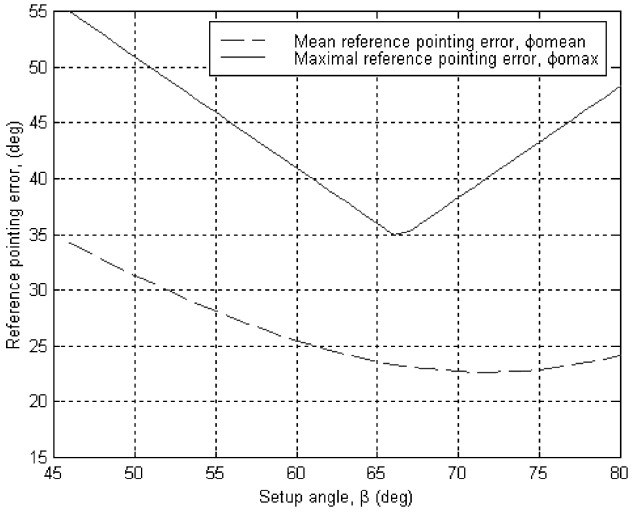

Fig. 2 Distributions of $\Phi_{0\max}$ and Φ_{0M} vs β.

Because the orbit of present constellation is sun synchronous, each satellite will pass over the accessible coverage zone about two times every day (one ascending and one descending). To have at least one satellite passing over this area per hour, there must be over 24 passes in one day, and at least 12 satellites are required for the constellation. The parameter T is assumed to be 12 up to the number that the coverage requirement is met. It is assumed that each orbital plane possesses one satellite; thus, the parameter P is equal to T. The value of phasing parameter F varies from 0 to $T-1$, and each phase represents one deployment of constellation. For example, the notation 14/14/0 represents 14 satellites at 14 orbital planes with the phasing angle $F=0$, and the first satellite in constellation is located at 0°E, 0°N as shown in Fig. 3. The access coverage of each satellite can be calculated by the ground track individually. The coverages of all satellites are arranged in time sequence of their appearances. Then the coverage gaps can be determined according to the definition of access coverage gap, and those gaps are labeled by the subscription k in sequence. The maximal and mean access coverage gaps can be calculated by substituting all of the gaps into Eqs. (4) and (5). Figure 4 shows the calculation results for the cases of $12/12/F$, $13/13/F$, and $14/14/F$. It shows that only the 14/14/0 constellation satisfactory meets the coverage requirement that $G_{\max}$ is less than one hour. The distributions of overall gaps of 14/14/0 constellation are shown in Fig. 5. It shows that all the gaps appeared at about 26 and 55 min alternately. Therefore one can obtain the weather images every 26 min and every 55 min alternately when the 14/14/0 constellation is employed.

Coverage in Latitude Band

Modification of Imagery System

Suppose there are j sets of cameras denoted as $S_1, S_2 \ldots S_j$, and $S_1, S_2 \ldots S_j$ are employed in the imagery system with different setup angles $\beta_1, \beta_2 \ldots \beta_j$, respectively. Each set of cameras includes two cameras set up each on the opposite side of the lateral of satellite with the same setup angle. In Ref. 5, it was found that the selection of setup angle of cameras only depends on the geomagnetic latitude of the imaging target. The setup angle of each set of cameras can be

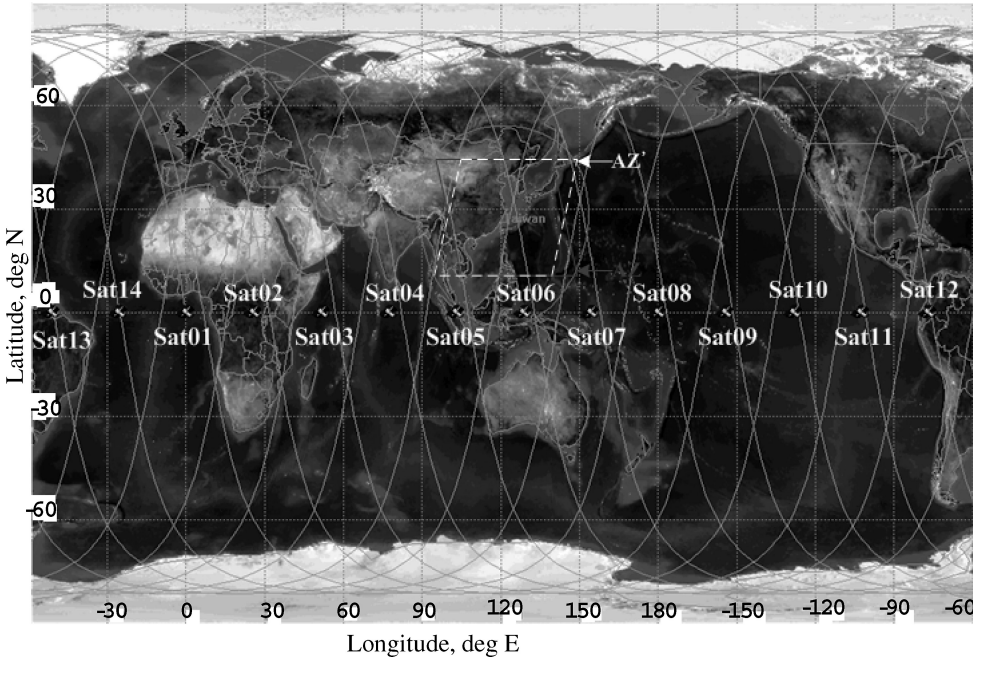

Fig. 3 Deployment of 14/14/0 constellation.

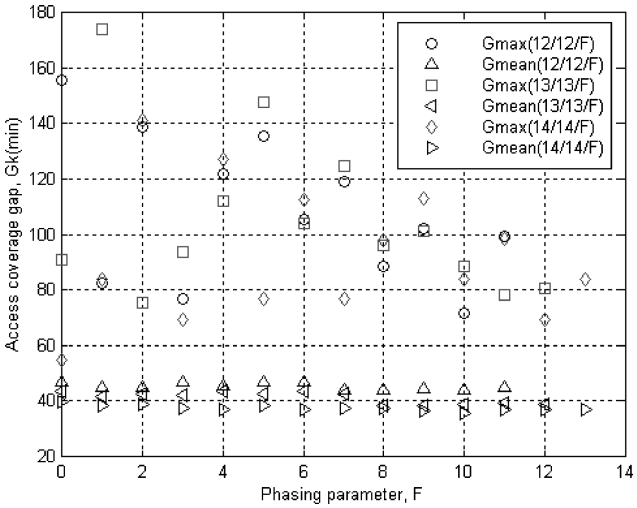

Fig. 4 $G_{\max}$ **and** G_{mean} **of the 12/12/*F*, 13/13/*F*, and 14/14/*F* constellations.**

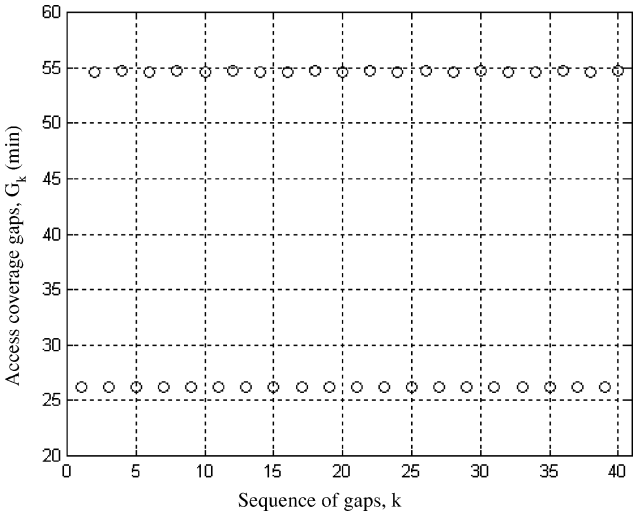

Fig. 5 Access coverage gaps of the 14/14/0 constellation.

determined by calculating the distributions of $\Phi_{0\max}$ vs θ_{m2}. Here, $S_1, S_2 \ldots S_j$ are adopted to acquire images of the targets located in the geomagnetic latitude bands, $B_1, B_2 \ldots B_j$ respectively, and satisfy the imaging requirement of Eq. (3) in $B_1, B_2 \ldots B_j$ respectively. When the target is located at B_1, camera S_1 is adopted; when the target is located at B_2, camera S_2 is adopted, and so on. Denote B_u as the union of $B_1, B_2 \ldots B_j$. The imagery system with multicameras can satisfy the imaging requirement for the area targets of the geomagnetic band B_u.

Coverage Band of 14/14/0 Constellation

Figures 6a and 6b is the distributions of $G_{\max}$ for the targets located in latitude band, which latitudes are between $\pm 60^\circ$N and longitudes are between 0°E to 360°E. It shows that $G_{\max}$ only relates to and is approximately linear proportional to the latitude. The relations between $G_{\max}$ and θ_{g2} can be expressed as

$$G_{\max} = 41 + 0.576|\theta_{g2}|, \qquad -60^\circ\text{N} \le \theta_{g2} \le 60^\circ\text{N} \tag{6}$$

The minimum $G_{\max}$ is 41 min at equator, and $G_{\max}$ is less than 60 min in the latitude band B_{la}, which latitudes are between $\pm 33^\circ$. The intersection of B_{la} and B_u is expressed as

$$B_s = B_{\text{la}} \cap B_u \tag{7}$$

In the area B_s, the imaging requirement and coverage requirements are both satisfied for the present 14/14/0 constellation. The constellation can provide one image per hour for the targets located at B_s.

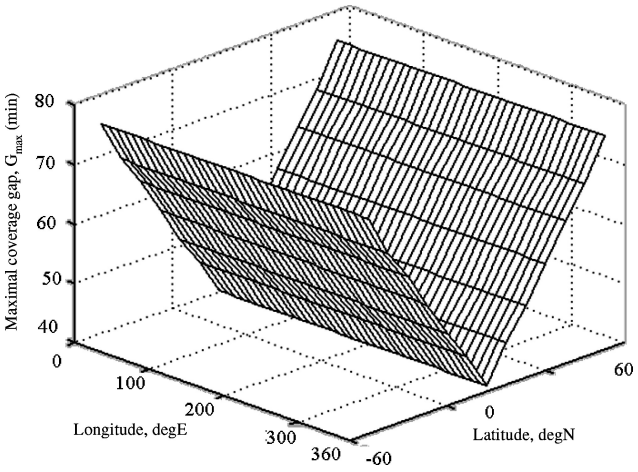

Fig. 6a $G_{\max}$ **of 14/14/0 constellation for the targets located in the latitude band** $\pm 60^\circ$**N.**

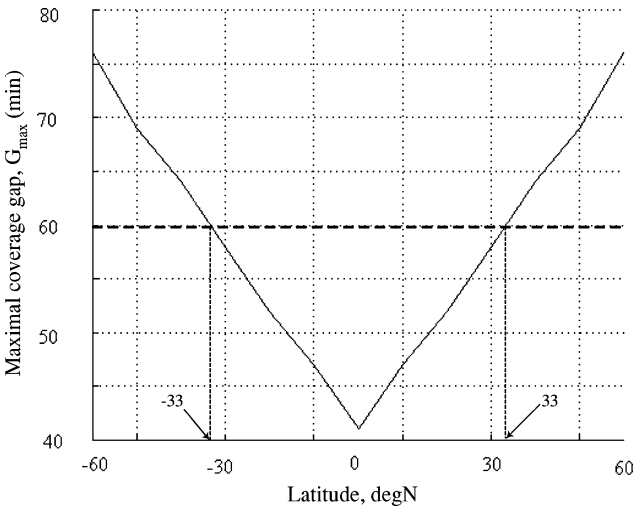

Fig. 6b Side view of Fig. 6a at latitude direction.

Example

We select the area target as $B_u = B_u(\theta_{m1}, \theta_{m2})$ ($0 \text{ deg} \le \theta_{m1} \le 360$ deg, $-5 \text{ deg} \le \theta_{m2} < 22$ deg), which includes Taiwan and the vicinity area where many typhoons occur every year. The criterion of choosing the setup angle of each camera set is to use the minimum number of camera sets to meet the imaging requirement of $\Phi_{0\max} \le 40$ deg in the geomagnetic latitude band B_u. The trial-and-error method, in which the value of β varies accordingly, is adopted to calculate the distributions of $\Phi_{0\max}$ vs θ_{m2}. As shown in Fig. 7, the calculation result indicates that the four camera sets combination of $\beta_1 = 91$ deg, $\beta_2 = 75$ deg, $\beta_3 = 63$ deg, and $\beta_4 = 56$ deg meets the imaging requirement of $\Phi_{0\max} \le 40$ deg in B_u. The corresponding bounds of the geomagnetic bands are given by

$$B_1 = B_1(\theta_{m1}, \theta_{m2}), \qquad 0 \text{ deg} \le \theta_{m1} \le 360 \text{ deg}$$
$$-5 \text{ deg} \le \theta_{m2} \le 3.9 \text{ deg} \tag{8a}$$

$$B_2 = B_2(\theta_{m1}, \theta_{m2}), \qquad 0 \text{ deg} \le \theta_{m1} \le 360 \text{ deg}$$
$$3.9 \text{ deg} < \theta_{m2} \le 12 \text{ deg} \tag{8b}$$

$$B_3 = B_3(\theta_{m1}, \theta_{m2}), \qquad 0 \text{ deg} \le \theta_{m1} \le 360 \text{ deg}$$
$$12 \text{ deg} < \theta_{m2} \le 18.1 \text{ deg} \tag{8c}$$

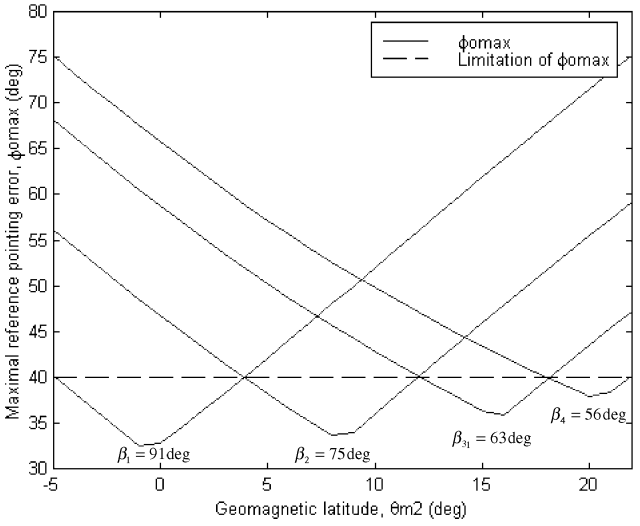

Fig. 7 $\Phi_{0\,max}$ of multicameras sets with different setup angles.

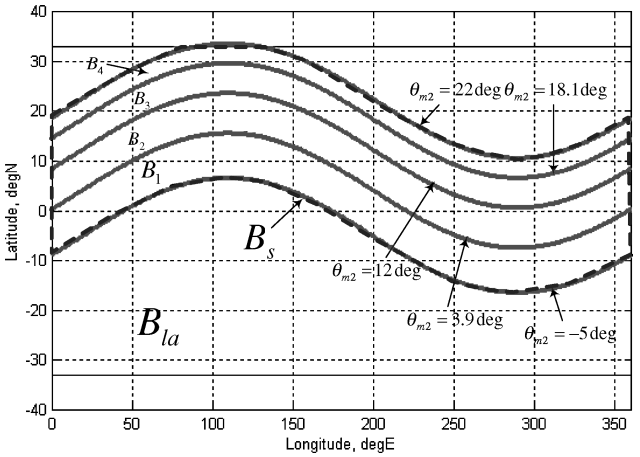

Fig. 8 Latitude band B_s that satisfies both the imaging and coverage requirements.

$$B_4 = B_4(\theta_{m1}, \theta_{m2}), \qquad 0 \text{ deg} \le \theta_{m1} \le 360 \text{ deg}$$
$$18.1 \text{ deg} < \theta_{m2} \le 22 \text{ deg} \tag{8d}$$

Figure 8 is the distributions of the latitude bands in the geographic coordinates. The dashed-line area B_s is the intersection of B_{la} and B_u that satisfies both the imaging and coverage requirements. The design of 14/14/0 constellation and the imagery system of multicameras of each satellite can acquire the weather images of the targets located in B_s per hour.

Application to Observe Typhoons

For the application to observe a typhoon, the 14/14/0 constellation and the imagery system of multicameras of each satellite presented in former section are employed. Figure 9 is the track of typhoon Toraji on 28–31 July 2001. In Fig. 9, we define the dashed-line area B_w as the warning area, in which the typhoons are possible to hit Taiwan. The warning area is determined according to the past tracks of typhoons over Taiwan from 1897 to 1966 that are provided by Central Weather Bureau,[10] Taiwan. Here, B_w is included in B_s and is expressed as

$$B_w = B_w(\theta_{g1}, \theta_{g2}), \qquad 115^\circ\text{E} \le \theta_{g1} \le 135^\circ\text{E}$$
$$16^\circ\text{N} \le \theta_{g2} \le 30^\circ\text{N} \tag{9}$$

Table 1 Simulation to observe typhoon Toraji

No. of acquiring images	Access started, h	Access stopped, h	θ_{g1} of target	θ_{g2} of target	No. of access satellite[a]
1	0.6669	0.83361	126.92	16.53	−13
2	1.6669	1.8336	126.92	16.53	+7
3	2.3669	2.5336	126.92	16.53	−14
4	3.3669	3.5336	126.92	16.53	+8
5	4.0336	4.2003	126.92	16.53	−1
6	5.0336	5.2003	126.41	16.724	+9
7	5.7336	5.9003	126.33	16.755	−2
8	6.7336	6.9003	126.21	16.799	+10
9	7.4003	7.5669	126.14	16.829	−3
10	8.4003	8.5669	125.02	16.873	+11
11	9.0669	9.2336	125.94	16.903	−4
12	10.1	10.267	125.82	16.949	+12
13	10.767	10.934	125.74	16.979	−5
14	11.767	11.934	125.63	17.023	+13
⋮	⋮	⋮	⋮	⋮	⋮
112	89.133	89.3	118.6	25.915	+2
113	89.733	89.9	118.55	25.975	−9
114	90.833	91	118.45	26.085	+3
115	91.4	91.567	118.4	26.142	−10
116	92.5	92.667	118.31	26.252	+4
117	93.1	93.267	118.25	26.312	−11
118	94.2	94.367	118.16	26.422	+5
119	94.767	94.933	118.11	26.479	−12
120	95.867	96.033	118.01	26.589	+6
121	96.467	96.633	117.99	26.665	−13
122	97.567	97.733	117.95	26.812	+7
123	98.133	98.3	117.93	26.887	−14
124	99.233	99.4	117.89	27.034	+8
125	99.833	100	117.87	27.114	−1
126	100.9	101.07	117.84	27.256	+9
127	101.5	101.67	117.82	27.336	−2
	$G_{\max} = 56$ min $G_{\text{mean}} = 37.638$ min				

[a]The − and + in last column represent descending and ascending respectively.

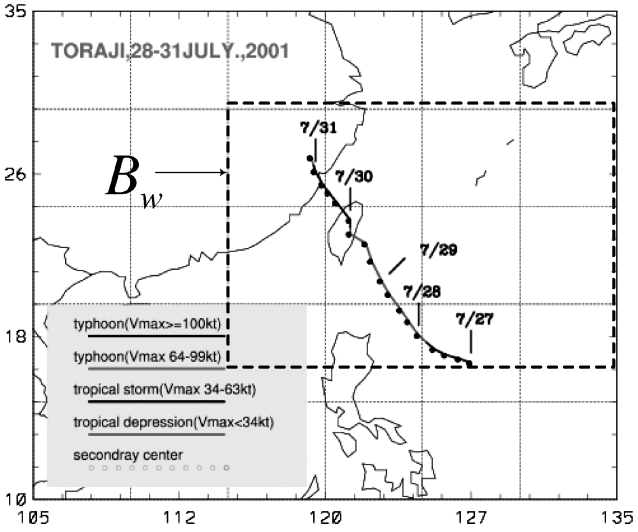

Fig. 9 Typhoon track of Toraji: – – –, area B_w defined as the warning area.

When the typhoon is crossing the edge of the warning area, the satellites of this constellation begin to take pictures continuously for 5 h. According to the former 5-h images, one predicts the path of typhoon for the next 5 h. Then employ the ground track to predict coverage data of the next 5 h and upload it to the satellites of this constellation. This tracking process will continue until the typhoon leaves the warning area. Table 1 is the simulation result of imaging opportunities to observe the typhoon Toraji show in Fig. 9 for the 14/14/0 constellation. The location of target is the same in the first 5 h

when the typhoon entered the warning area on 27 July. The location of target and the access coverage of constellation in the next 5 h are predicted according to the data of the former 5 h. The 15–111 imaging opportunities in Table 1 continuously repeat the prediction progress and are not presented in Table 1 to avoid tediousness. This prediction progress is continued until the typhoon Toraji dissipated on 31 July. The maximal coverage gap is 56 min, and the mean coverage gap is 37.638 min. It shows that there are 127 images acquired during 102 h and satisfies the mission requirement of at least one image acquired per hour.

The present design can be easily applied, with little modification, to observe any significant moving targets on the other place of the world within the geomagnetic latitude band B_s. If the intersatellite-link devices were employed and the remote-sensing technique was improved in the constellation of satellites, one can also observe a moving target in the same geomagnetic latitude band around the Earth closely real time. This observing band could also be expanded to include more places of the world if double constellations or a hybrid constellation were adopted.

Conclusions

The constellation constituted by 14 low-cost satellites to acquire the weather images of Taiwan hourly is presented. The 14/14/0 Walker constellation was also extended to acquire the images of targets located in certain specified latitude band hourly, with the modification of imagery system. The application to observe typhoons as the moving targets in the warning area of Taiwan was also presented. The simulation results of observing the typhoon Toraji shows that 127 images can be obtained during 102 h.

Acknowledgment

The research was supported by Nation Science Council of Taiwan, Republic of China, under Contract NSC-91-2213-E-032-007.

References

[1]White, J., "Microsat Motion, Stabilization, and Telemetry," *Radio Amateur Satellite Corporation-North America Journal*, Vol. 13, No. 4, 1990, pp. 13–30.

[2]Lu, R. A., Olsen, T. A., and Swartwout, M. A., "Building 'Small, Cheaper, Faster' Satellites Within the Constraint of an Academic Environment," 9th Annual AIAA/USU Conf. on Small Satellites, Poster Session, Sept. 1995.

[3]Menges, B. M., Guadiamos, C. A., and Lewis, E. K., "Dynamic Modeling of Micro-Satellite Spartnik's Attitude," Region VI AIAA Student Conf., April 1997.

[4]Ovchinnikov, M., and Pen'kov, V., "Attitude Control System for The First Swedish Nanosatellite MUNIN," *Acta Astronautica*, Vol. 46, Nos. 2–6, 2000, pp. 319–326.

[5]Hong, Z. C., Lin, C. H., and Lin, H. J., "Imagery Payload Design for Passive Magnetically Stabilized Microsatellite," *Journal of Spacecraft and Rockets*, Vol. 40, No. 3, 2003, pp. 396–404.

[6]Lin, C. H., Shih, C. H., and Chuang, C. K., "The Passive Magnetic Stabilization used Magnetic Rods for a Microsatellite TUU SAT-1," International Astronautical Federation, Paper IAF-ST-99 -W.1.06, Oct. 1999.

[7]Hong, Z. C., Lin, C. H., and Chang, W. C., "The Design and Analysis of Magnetic Attitude Control System for Micro-Satellite," Final Rept. of National Science Council, NSC-90-2213-E-032-009, Taipei, Aug. 2002.

[8]Moshe, B. L., Leonid, S., and Vola, L., "EROS System-Satellite Orbit and Constellation Design," *Proceedings of the 22nd Asian Conference on Remote Sensing*, Vol. 2, CRISP, Singapore, 2001, pp. 1153–1158.

[9]Lang, T. J., and William, S. A., "A Comparison of Satellite Constellation for Continuous Global Coverage," *Proceedings of the Mission Design and Implementation of Satellite Constellations*, edited by J. C. van der Ha, Vol. 1, Kluwer Academic, Dordrecht, The Netherlands, 1997, pp. 51–62.

[10]Shieh, S. L., Wang, S. T., Cheng, M. D., Yeh, T. C., and Chiou, T. K., "User's Guide for Typhoon Forecasting in the Taiwan Area (VII)," Atmospheric R&D Center, Central Weather Bureau, Technique Rept. CWB87-1M-01, Taipei, June 1998, p. 171.

D. Spencer
Associate Editor